# Fischer-Tropsch synthesis over $Co/TiO_2$ catalyst: effect of catalyst activation by CO compared to $H_2$

Kalala Jalama

Department of Chemical Engineering, University of Johannesburg, P.O. Box 17011, Doornfontein 2028, Johannesburg, South Africa, e-mail: kjalama@uj.ac.za

## Abstract

$Co/TiO_2$ catalyst activation for Fischer-Tropsch (FT) reaction by CO in comparison to $H_2$ has been performed. The catalyst, prepared by incipient wetness impregnation, has been characterized using X-ray diffraction (XRD) and X-ray photoelectron spectroscopy (XPS) analyses after separate reduction using CO and $H_2$ respectively. Temperature programmed reduction (TPR) analyses were also conducted to study the reduction behaviour of the catalyst in presence of $H_2$ and CO respectively. CO improved catalyst reduction and produced a more stable and active catalyst with higher selectivity and yield for $C_{5+}$ hydrocarbons at extended time-on-stream.

*Keywords*: Catalyst activation; CO; $H_2$; Fischer-Tropsch

## 1. Introduction

Fischer-Tropsch (FT) synthesis is a process that converts synthesis gas into liquid fuel over metal catalysts. Supported cobalt, fused iron and precipitated iron catalysts are the most used in commercial applications [1]. An activation process that consists of reducing the cobalt oxides particles in the catalyst to metallic cobalt is always required prior to the FT reaction. $H_2$ is usually used to activate cobalt catalysts at 250-400$^oC$ [1]. This standard catalyst activation is usually limited by some interaction between the support and cobalt. Cobalt-support compounds formation have been reported to form in supported cobalt catalysts during activation using $H_2$ [2-7]. Jongsomjit *et al*. [7] reported the formation of Co-titanate during standard reduction of a $Co/TiO_2$ catalyst

using $H_2$. The formed compound cannot be reduced below 800$^oC$ and limits the degree of reduction for the catalyst. In some cases, the formation of these cobalt-support compounds is influenced by the presence of water produced during the reduction process [3]. Only a limited amount of literature has reported to date on cobalt catalyst activation process that does not involve water formation. Li *et al*. [8] used CO to activate a ruthenium-promoted $Co/TiO_2$ catalyst at 523 K and 1.68 MPa and compared its performance for FT reaction with an $H_2$-activated catalyst. They measured lower activity and good stability on the CO-reduced catalyst. Pan and Bukur [9] reduced Co/ZnO catalyst with CO at 523 K and measured lower activity and olefin content, and more methane compared to the $H_2$-reduced sample. These predominantly negative effects of cobalt catalyst activation by CO on the FT reaction performance could most likely be due to the low temperature and high CO partial pressure used for catalyst activation. Cobalt carbide and CoO were the major phases in the catalyst sample reduced by CO at 523 K [9].

To the best of our knowledge, there is no other report on the effect of activating cobalt-based catalyst with CO, under conditions that avoid cobalt carbide formation, on catalyst performance for FT reaction. Hence the aim of this study is to investigate the effect of $Co/TiO_2$ catalyst activation by diluted CO (5%CO in He) at 350$^oC$ on FT reaction performance.

## 2. Experimental procedure

### 2.1 Catalyst preparation and characterization

The details on catalyst preparation are reported in earlier studies [10, 11].

Temperature programmed reduction (TPR) was performed using 100 mg of fresh $Co/TiO_2$ catalyst sample. Bulk $Co_3O_4$ samples (10 mg) were also used to facilitate

reduction peak identification. The sample was first degassed at 150 $^{o}$C in a flow of Ar (30 Nml/min) for 45 minutes and then cooled to 60 $^{o}$C before replacing the Ar flow with the analysis gas (5% $H_2$ in Ar or 5%CO in He, 30 Nml/min) to start the TPR analysis. The temperature was increased at a rate of 10$^{o}$C/min.

X-ray diffraction (XRD) analysis was carried out using Rigaku Ultima IV X-ray powder diffractometer with PDXL analysis software. The following analysis parameters were used: Cu-Kα (λ = 1.54 Å) radiation source, current and voltage set at 30 mA and 40 KV and step width of 2θ = 0.01$^{o}$.

X-ray photoelectron spectroscopy (XPS) analysis was performed using a Kratos Axis Ultra DLD system. The following settings were used: monochromatic Al Ka X-ray source operating at 120 W; pass energies of 160 eV for survey spectra; 40 eV for high resolution scans; hybrid operation mode using a combination of magnetic immersion and electrostatic lenses; acquisition area of approximately 300 x 700 $\mu m^2$; take off angle of 90° and a base pressure of ca. $1x10^{-9}$ Torr.

### 2.2 Catalyst evaluation

500 mg of fresh catalyst (particles with sizes between 0.5 and 1 mm) were loaded in a fixed-bed stainless steel reactor (internal diameter: 16 mm, length: 260 mm) and dried at 150 $^{o}$C in a flow of $N_2$ (30 Nml/min) for 60 min before exposure to the reducing gas mixture. Catalyst reduction was done at 350$^{o}$C (heating rate: 10$^{o}$C/min) for 14 hours using 5%$H_2$ in Ar or 5%CO in He (30 Nml/min) at atmospheric pressure.

FT runs were performed at 220$^{o}$C, 20 bar using a premixed gas with $H_2$:CO ratio of ca. 2 and a feed flowrate of ca. 10 Nml/min. The outlet gas stream was analysed by online gas chromatography using a Supel-Q Plot fused silica capillary column 30 m x 0.32 mm and a stainless steel general 60/80 Carboxen 1000.

## 3. Results and discussion

### 3.1 Catalyst characterization

The data for TPR analysis using $H_2$ or CO are summarized in fig. 1.

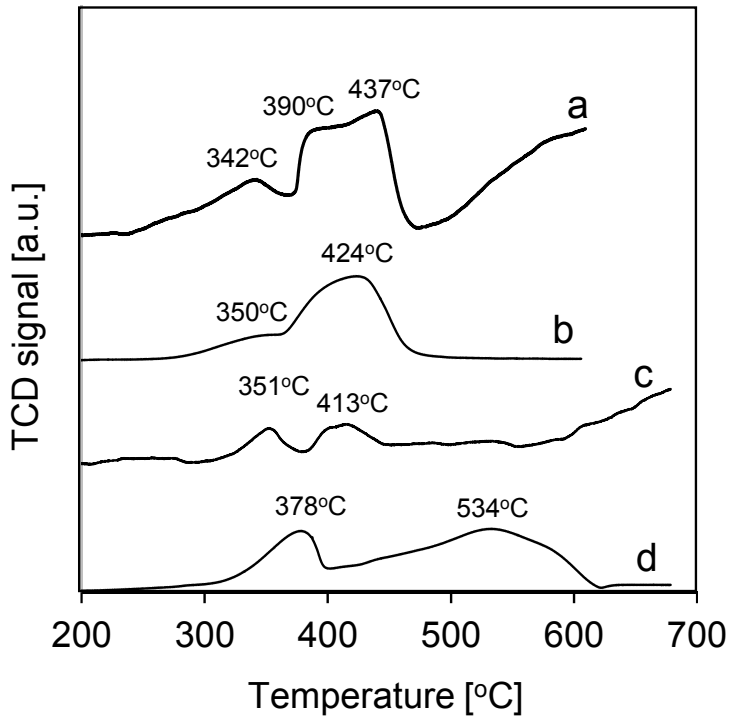


**Fig. 1.** TPR data for bulk $Co_3O_4$ using a) CO; b) $H_2$, and for $Co/TiO_2$ sample using c) CO and d) $H_2$.

The first reduction peak for bulk $Co_3O_4$ in presence of CO (fig. 1a) started from ca. 237°C and reached its maximum value at ca. 342°C. It can be attributed to the first reduction step of $Co_3O_4$ to CoO. A second peak starting at ca. 370°C showed a rapid CO consumption rate up to a temperature of 390°C after which an almost steady CO consumption rate was observed up to ca. 407°C followed by a maximum value at ca. 437°C. This peak can be attributed to the reduction of CoO to $Co^0$. The peak starting at ca. 480°C is attributed to significant carbon deposition. In presence of $H_2$, the bulk

$Co_3O_4$ sample (fig. 1b) showed two peaks with maximum values at ca. 350 and 424°C attributed to the two-step reduction of $Co_3O_4$ to Co and $Co^0$. The data show that bulk $Co_3O_4$ can be reduced by CO or $H_2$ in a similar temperature range. The data for the supported catalyst in presence of CO (fig. 1c) also showed two peaks with their maxima at ca. 351 and 413°C respectively. These peaks, also attributed to the two-step reduction of $Co_3O_4$ to CoO and $Co^0$, are well in the same temperature range as that required for the reduction of bulk $Co_3O_4$. However, a delayed peak for carbon deposition was only observed from ca. 560°C compared to 480°C in the case of bulk $Co_3O_4$. The role of the $TiO_2$ support in delaying carbon deposition is unclear and will require future investigation. A significant shift of reduction peaks to higher temperatures was observed for the TPR analysis of the $TiO_2$-supported cobalt catalyst sample using $H_2$ (fig. 1d). The first reduction peak, attributed to the first reduction step of $Co_3O_4$ to CoO reached its maximum at ca. 378°C compared to 351°C in the presence of CO (fig. 1c). In addition, a broad reduction peak with maximum at ca. 534°C and extending up to ca. 620°C suggests the second reduction step of cobalt species with various levels of interaction with the $TiO_2$ support to $Co^0$. These data suggest that reduction using $H_2$ leads to strong cobalt-titania interactions in the catalyst compared to CO. It is possible that the latter prevented or limited these interactions in the catalyst during the reduction process to improve catalyst reducibility. Previous studies [5, 11] have also reported improved cobalt catalyst reduction due to the presence of CO in the reducing gas.

XRD analyses were performed to confirm the cobalt phases that were present in the catalyst after reduction with CO or $H_2$ at 350°C for 14 hours as described in section 2.2. The samples were cooled to room temperature under the flow of the reducing gas and passivated using 5% $O_2$ in He for 30 min. Some portions of the passivated

samples were also sent for XPS analysis. Diffraction patterns for $H_2$-reduced (fig. 2a) and CO-reduced (fig. 2b) samples were similar and both showed CoO and $Co^0$ as major cobalt phases.

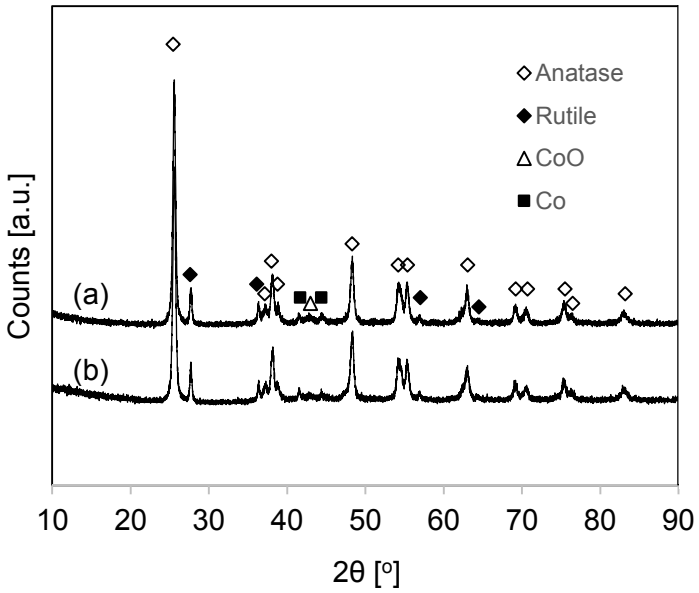


**Fig. 2.** XRD data for $Co/TiO_2$ catalyst after reduction with a) $H_2$; b) CO

Different from other studies [8, 9, 12], no cobalt carbide was detected in CO-reduced samples as shown by XRD data. A separate analysis was performed on the TPR apparatus by heating a CO-reduced catalyst sample to 350°C in a flow of $H_2$ (5%$H_2$ in Ar) in order to convert any cobalt carbide to Co metal and methane or light hydrocarbons respectively. The outlet of the TPR reactor was connected to an FID for possible methane/hydrocarbon detection. No peak was detected.

XPS analyses were performed to supplement TPR and XRD data, and determine the surface composition of $H_2$- and CO-reduced catalyst samples.

C 1s data (fig. 3a) for both $H_2$- and CO-reduced catalyst samples were similar with a major peak at 284.8 eV due to adventitious carbon.

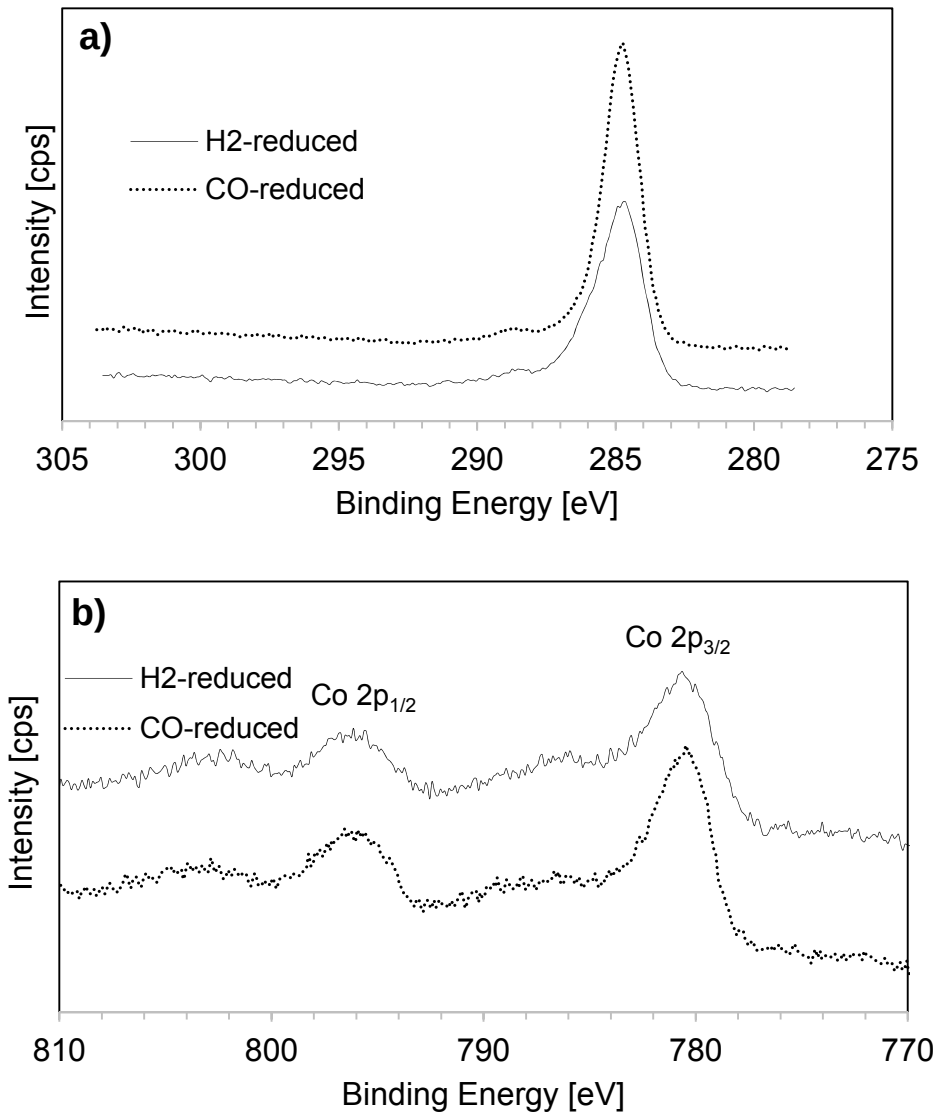


**Fig. 3**. XPS data for a) C 1s and b) Co 2p

Carbidic carbon peak has been reported to occur at ca. 282.5 eV [13]. This peak was not observed in the data reported in fig. 3 and confirms, in agreement with XRD data and FID analysis, that catalyst reduction with diluted CO did not lead to cobalt carbide formation.

Most studies have performed cobalt carburization using CO at higher pressures [8, 12, 14, 15] and lower temperatures compared to the conditions selected in this study. Li *et al*. [8] and Yang *et al.* [12] used a pressure of 1.68 MPa and a temperature of 523

K to carburize a Ru-promoted $Co/TiO_2$ catalyst in CO. Karaca *et al.* [14] and Kwak *et al*. [15] carburized a reduced $CoPt/Al_2O_3$ catalyst at 2.0 MPa and 220°C in a flow of pure CO.

The overall $Co_3O_4$ carburization with CO can be written as

$$2Co_3O_4 + 14CO \rightarrow 3Co_2C + 11CO_2 \quad (1)$$

The reaction proceeds with gas contraction and is thermodynamically favoured at higher pressures. Very low pressure for CO (5% CO in He at atmospheric pressure) was selected in this study in order to avoid or limit cobalt carbide formation. These observations are in agreement with Liotta *et al*. [16] who also reported reduction of $Co_3O_4$ to CoO and subsequently to Co metal during TPR analysis of a $Co/Al_2O_3$-BaO catalyst using a low CO pressure (1%CO in He).

$H_2$- and CO-reduced catalyst samples displayed similar Co 2p spectra (fig. 3b). Peaks for Co $2p_{3/2}$ and Co $2p_{½}$ were detected at 780.6 and 796.5 eV respectively. Satellite peaks for Co $2p_{3/2}$ and Co $2p_{½}$ were also observed at 786.6 and 802.8 eV respectively and suggested that cobalt was present on both $H_2$- and CO-reduced catalyst surface as CoO [17]. Surface atomic compositions for the catalyst samples are reported in table 1.

**Table 1**

Catalyst surface composition determined by XPS

| Catalyst | Surface atomic % | | | Co/Ti atomic ratio |
|---|---|---|---|---|
| | Co 2p | O 1s | Ti 2p | |
| $H_2$-reduced catalyst | 5.73 | 68.07 | 26.20 | 0.22 |
| CO-reduced catalyst | 6.99 | 68.10 | 24.91 | 0.28 |

CO-reduced catalyst had 6.99% of surface cobalt compared to 5.75% for the $H_2$-reduced sample. Also the Co/Ti ratio of 0.28 after reduction using CO was higher than 0.22 measured after reduction using $H_2$. These data indeed suggest that catalyst reduction with CO leads to high cobalt dispersion on the catalyst surface.

### 3.2 Catalyst evaluation

The performance of $H_2$- and CO-reduced catalysts for FT reaction has been compared at early and extended time on stream (TOS). CO conversion and methane selectivity as function of TOS are reported in fig. 4. Averaged values are reported in table 2.

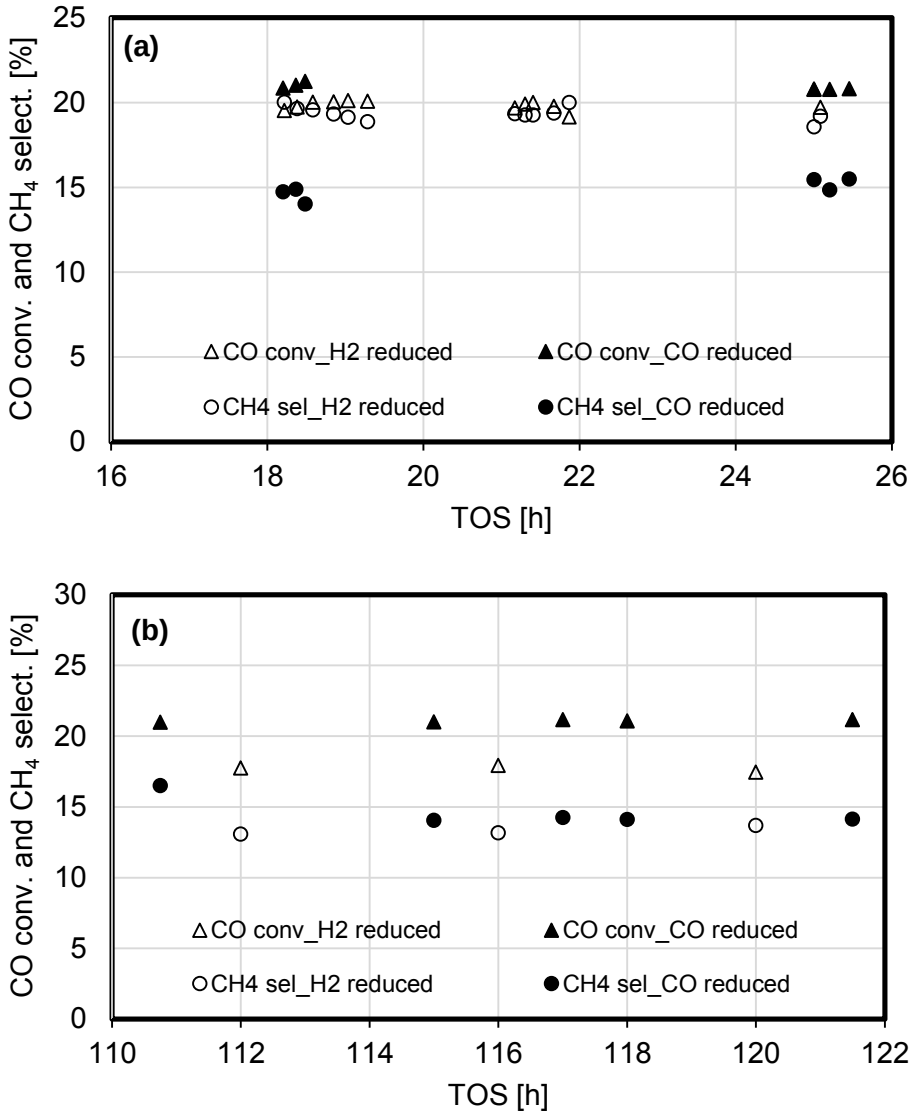

**Fig. 4.** CO conversion and methane selectivity over $Co/TiO_2$ catalyst reduced using $H_2$ and CO respectively at a) early TOS and b) extended TOS

## Table 2

Summary FT data

| Run details | CO conv. [%] | -rCO [mol/$g_{Cat}$/h] | $rCH_4$ [mol/$g_{Cat}$/h] | $CH_4$ select. [%] | $C_2$-$C_4$ select. [%] | $C_{5+}$ select. [%] | $rC_{5+}$ [mg/$g_{Cat}$/h] | Alpha* | Olefin to paraffin ratio* | | | | | | |
|---|---|---|---|---|---|---|---|---|---|---|---|---|---|---|---|
| | | | | | | | | | 3 | 4 | 5 | 6 | 7 | 8 | Overall** |
| ***Early TOS (< 30h)*** | | | | | | | | | | | | | | | |
| $H_2$-reduced catalyst | 19.9 ± 0.4 | 0.00333 | 0.00064 | 19.4 ± 0.4 | 26.8 | 53.8 | 25.1 | 0.73 | 0.80 | 0.49 | 0.57 | 0.41 | 0.26 | | 0.29 |
| CO-reduced catalyst | 20.9 ± 0.2 | 0.00350 | 0.00052 | 14.9 ± 0.5 | 14.8 | 70.2 | 34.4 | 0.91 | 0.99 | 0.52 | 0.58 | 0.39 | 0.31 | 0.21 | 0.28 |
| ***Extended TOS (>100h)*** | | | | | | | | | | | | | | | |
| $H_2$-reduced catalyst | 17.6 ± 0.3 | 0.00294 | 0.00040 | 13.5 ± 0.4 | 24.7 | 61.7 | 25.4 | 0.67 | 1.55 | 0.80 | 1.25 | 0.88 | 0.73 | 0.55 | 0.59 |
| CO-reduced catalyst | 21.1 ± 0.1 | 0.00352 | 0.00051 | 14.6 ± 1.1 | 16.4 | 69.0 | 34.0 | 0.92 | 1.04 | 0.53 | 0.60 | 0.38 | 0.33 | 0.25 | 0.30 |

*based on gas product

**w eight based

At early TOS, $H_2$- and CO-reduced catalyst samples had comparable CO conversions of ca. 20 and 21% respectively. This was not expected since better catalyst reduction and higher cobalt dispersion (as indicated by Co/Ti ratio from XPS analysis) were obtained when the catalyst was activated by CO. This would lead to high active sites density in the catalyst resulting in significantly higher conversion. Thus, the observed data suggest that the *specific* FT activity at early TOS was higher for the $H_2$-reduced sample, possibly due the strong metal support interaction (SMSI) in the catalyst [18] compared to the CO-reduced catalyst. However, higher methane selectivity of ca. 19% was measured on the $H_2$-reduced catalyst compared to ca. 15% for the CO-reduced catalyst. A decline in CO conversion rate from 0.00333 to 0.00294 mol/$g_{Cat}$/h (ca. 12% activity loss) and methane selectivity from 19.4 to 13.5% was observed for $H_2$-reduced catalyst sample at extended TOS. The CO-reduced catalyst showed more stability as the CO conversion rate and methane selectivity at early and extended TOS were comparable.

Fig. 5 shows the gas phase product distribution for both $H_2$- and CO-reduced catalysts at early and extended TOS and their corresponding alpha values in table 2. Up to $C_8$ hydrocarbons were detected in the gas product after a cold trap at room temperature. The product distribution for the CO-reduced catalyst was practically the same at both early and extended TOS with the corresponding alpha values of 0.91 and 0.92 respectively. The $H_2$-reduced catalyst had alpha values of 0.73 and 0.67 at early and extended TOS respectively.

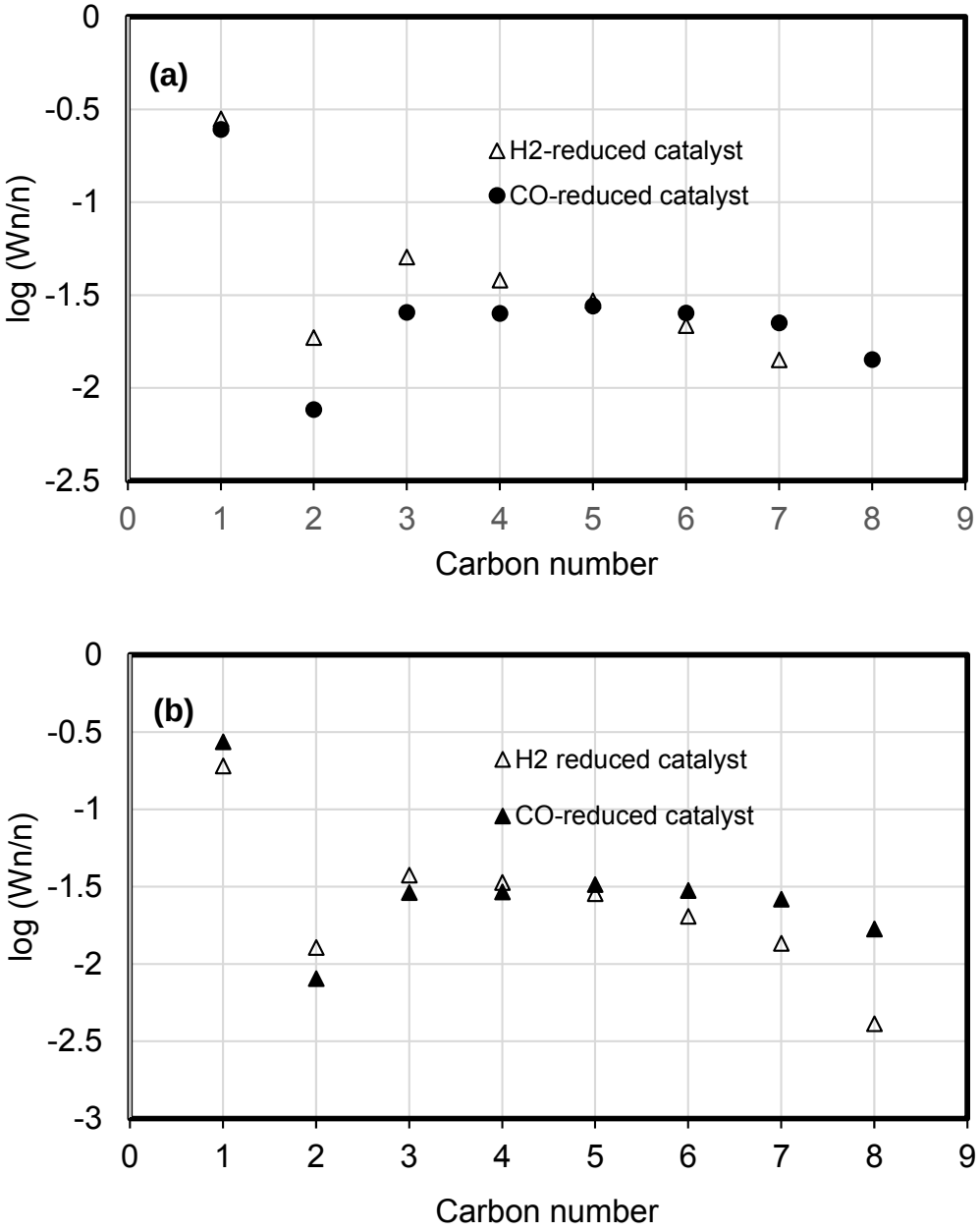


**Fig. 5.** Light hydrocarbons distribution (based on gas product) over $H_2$- and CO-reduced catalyst at a) early reaction times and b) extended reaction times.

Overall olefin to paraffin ratios (table 2) at early TOS were comparable and around 0.28 and 0.29 for CO- and $H_2$-reduced catalysts respectively but shifted to a higher value (doubled) for the $H_2$-reduced catalyst at extended TOS. Catalyst evaluation data, as summarized in table 2 show that reduction with CO produces a more stable and active catalyst that reaches steady state faster with higher $C_{5+}$ selectivity (69%) and

production rate of 34 mg/gCat/h at extended TOS compared to 61.7% and 25.4 mg/Cat/h for $H_2$-reduced catalyst. Li *et al*. [8] also observed that cobalt-based catalyst pre-treated with CO reaches a steady state faster and is stable.

Concomitantly with the decline in $H_2$-reduced catalyst activity at extended TOS, the following observations can be summarized from the data in table 2: i) decline in methane formation rate from 0.00064 to 0.00040 mol/$g_{Cat}$/h (ca. 38% decline); ii) increase in overall olefin to paraffin ratio (double) and iii) steady rate for $C_{5+}$ formation which remained unchanged around 25 mg/gCat/h. These observations suggest a decline in the density of catalytic sites which are more selective for hydrogenation and $CH_4$ formation. It has been proposed that SMSI leads to a raft-like morphology of metal on a $TiO_2$ support [19]. Plane sites have been visualized to possess specificity for hydrogenation and are significantly poisoned by strong CO adsorption during FT reaction [20].

## 4. Conclusion

Different from previous studies which reported negative effect of cobalt catalyst activation by CO, this study used significantly lower partial pressure of CO and a higher temperature for the reduction process. Under these conditions, no cobalt carbide was detected. CO or $H_2$ led to different types of interactions of cobalt species and the $TiO_2$ support which led to differences in catalyst reducibility and performance for FT reaction. CO improved catalyst reduction and produced a more stable and active catalyst with higher selectivity and yield for $C_{5+}$ hydrocarbons at extended TOS compared to the $H_2$-reduced catalyst.

**Acknowledgements**

Financial support from the National Research Foundation (NRF) and the University of Johannesburg is acknowledged.

Cardiff Institute of Catalysis is also acknowledged for assistance with XPS analyses.

**References**

[1] A. Steynberg, M. Dry, Studies in Surface Science and Catalysis 152 (2004) 533.

[2] A. Kogelbauer, J.C. Weber, J.G. Goodwin Jr., Catalysis Letters 34 (1995) 259.

[3] Y.Zhang, D. Wei, S. Hammache, J.G. Goodwin Jr., Journal of Catalysis 188 (1999) 281.

[4] B. Jongsomjit, J. Panpranot, J.G. Goodwin Jr., Journal of Catalysis 204 (2001) 98.

[5] B. Jongsomjit, J.G. Goodwin Jr., Catalysis Today 77 (2002) 191.

[6] B. Jongsomjit, J. Panpranot, J.G. Goodwin Jr., Journal of Catalysis 215 (2003) 66.

[7] B. Jongsomjit, C. Sakdamnuson, J.G. Goodwin Jr, P. Praserthdam, Catalysis Letters 94 (2004) 209.

[8] J Li, L. Xu, R. Keogh, B. Davis, Catalysis Letters 70 (2000) 127.

[9] Z. Pan, D.B. Bukur, Applied Catalysis A: General 404 (2011) 74.

[10] K. Jalama, N.J. Coville, D. Hildebrandt, D. Glasser, L.L. Jewell, Fuel 86 (2007) 73.

[11] K. Jalama, J. Kabuba, H. Xiong, L.L. Jewell, Catalysis Communications 17 (2012) 154.

[12] J. Yang, G. Jacobs, T. Jermwongratanachai, V.R.R. Pendyala, W. Ma, D. Chen, A. Holmen, B.H. Davis, Catalysis Letters 144 (2014) 123.

[13] D.-X. Ye, S. Pimanpang, C. Jezewski, F. Tang , J.J. Senkevich, G.-C. Wang, T.-M. Lu, Thin Solid Films 485 (2005) 95.

[14] H. Karaca, O.V. Safonova, S. Chambrey, P. Fongarland, P. Roussel, A. Griboval-Constant, M. Lacroix, A.Y. Khodakov, Journal of Catalysis 277 (2011) 14.

[15] G. Kwak, M.H. Woo, S.C. Kang, H-G. Park, Y-J. Lee, K-W. Jun, K-S. Ha, Journal of Catalysis 307 (2013) 27.

[16] L.F. Liotta, G. Pantaleo, G. Di. Carlo, G. Marci, G. Deganello, Applied Catalysis B: Environmental 52 (2004) 1.

[17] Sarah C. Petitto, Erin M. Marsh, Gregory A. Carson, Marjorie Langell, Journal of Molecular Catalysis A: Chemical 281 (2008) 49.

[18] R.C. Reuel and C.H. Bartholomew, Journal of Catalysis 85 (1984) 78.

[19] J.S. Smith, P.A. Thrower, M.A. Vannice, Journal of Catalysis 68 (1981) 255.

[20] H. Schulz, Z. Nie, F. Ousmanov, Catalysis Totay 71 (2002) 351.